

Directed supramolecular assembly of Cu(II)-based “paddlewheels” into infinite 1-D chains using structurally bifunctional ligands

Christer B. Aakeröy,* Nate Schultheiss and John Desper

Received 28th September 2005, Accepted 23rd November 2005

First published as an Advance Article on the web 6th December 2005

DOI: 10.1039/b513765a

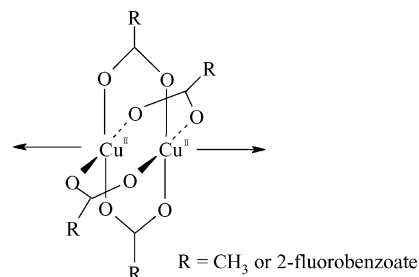
The construction of Cu(II)-containing supramolecular chains is achieved by combining suitable anionic ligands (for controlling the coordination geometry and for creating a neutral building block) with four new bifunctional ligands containing a metal-coordinating pyridyl site and a self-complementary hydrogen-bonding moiety. Seven crystal structures are presented and in each case, the copper(II) complex displays a “paddlewheel” arrangement, with four carboxylate ligands occupying the equatorial sites, leaving room for the bifunctional ligand to coordinate in the axial positions. The supramolecular chemistry, which organizes the coordination-complexes into the desired infinite 1-D chains, is driven by a combination of N–H⋯N and N–H⋯O hydrogen-bonds in five of the seven structures.

Introduction

The design and synthesis of inorganic–organic hybrid materials with desired topologies, through supramolecular synthesis, is a rapidly emerging field within crystal engineering.¹ The ability to translate the inherent dimensionality and geometry of any coordination complex into extended architectures with specific (and tunable) metrics is critical in producing materials with desired chemical and physical properties.² The use of coordinate covalent bonds for the assembly of coordination polymers is well established,³ whereas supramolecular synthetic strategies that utilize non-covalent (*i.e.* hydrogen bonds,⁴ π – π interactions,⁵ *etc.*) and metal–ligand interactions within the same network are far less developed.⁶ Composite hybrid materials are of crucial importance in natural systems⁷ and they have also found numerous uses in synthetic high-tech applications.⁸ The combination of organic ligands and coordination chemistry also brings together synthetic flexibility (from principles of organic chemistry) and properties and reactivities inherent in many transition-metal ions. Thus, the ability to reliably prepare new extended hybrid materials with desirable structures from soluble precursors remains a very important target in synthetic and materials chemistry.

We are particularly interested in identifying systems that simplify the supramolecular assembly which means that we need to (a) carefully control the geometry of the complex ion and, (b) eliminate the need for potentially disruptive counterions. This is particularly important when targeting metal ions with diverse and unpredictable coordination modes such as Cu(II). With this in mind, a variety of structurally bifunctional organic ligands containing a metal-ion coordinating moiety and a hydrogen bonding functionality were synthesized with the specific supramolecular goal of organizing a variety of Cu(II)-based complex ions into infinite 1-D chains. Dinuclear Cu(II) complexes incorporating four carboxylate moieties ($\text{Cu}^{\text{II}}_2\text{L}_4$, where L = acetate or 2-fluorobenzoate) provide a reasonable starting point since the four monoanionic functional groups bridge two copper(II) centers

thereby creating a neutral “paddlewheel” complex, Scheme 1. Each copper ion is in an arrangement where four of the equatorial positions are coordinated by the anions, leaving a vacant axial position accessible for the supramolecular ligand.



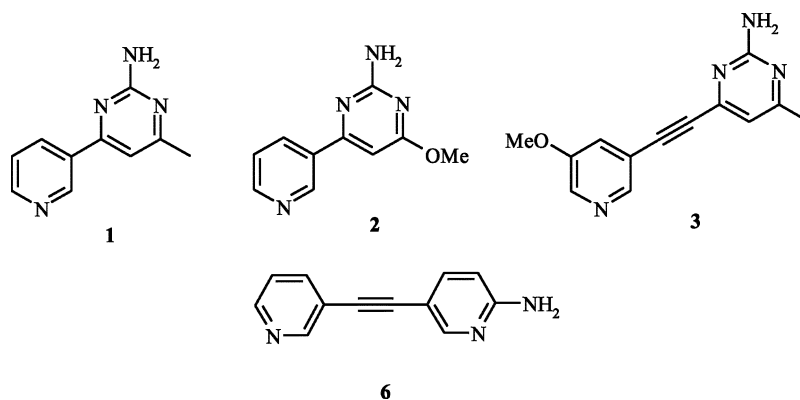
Scheme 1 Substituted “paddlewheel” complex with arrows showing the two axial coordination sites.

A structurally bifunctional ligand (a supramolecular linker) for this family of complex ions could combine a donor atom capable of effective metal-ion coordination with a functional group capable of forming self-complementary hydrogen bonds to a neighboring complex, thus extending the network. Four different ligands were designed and synthesized to fit these specific requirements, Scheme 2.

Ligands **1** and **2** have slightly dissimilar hydrogen-bonding moieties due to the differences in electronic and steric influences provided by the methyl and methoxy substituents, respectively. In contrast, ligands **3** and **6** contain an ethynyl linker between the two heterocyclic rings, allowing for greater separation between the metal-ions within each chain, which provides a handle for tuning some potentially important metrics of the resulting architecture. Ligand **6** contains an amino-pyridine fragment instead of an amino-pyrimidine unit but it is still capable of forming self-complementary hydrogen-bond interactions with ligands of neighboring complex ions.

In this study, we outline a specific and predetermined supramolecular design strategy for the construction of 1-D chains from suitable bifunctional organic ligands **1,2,3,6** and dinuclear copper(II) acetate or copper(II) 2-fluorobenzoate complex ions.

Department of Chemistry, Kansas State University, Manhattan, Kansas, 66506, USA. E-mail: aakeroy@ksu.edu



Scheme 2 A family of structurally bifunctional ligands; 3-(2-amino-4-methylpyrimidin-6-yl)pyridine **1**, 3-(2-amino-4-methoxypyrimidin-6-yl)pyridine **2**, 1-(2-amino-4-methylpyrimidin-6-yl)-2-(3-methoxypyridin-5-yl)ethyne **3**, 1-(2-aminopyrid-5-yl)-2-(pyrid-3-yl)ethyne **6**.

The reliability of the assembly process is evaluated by an examination of seven crystal structures in the context of the desired supramolecular target and the primary intermolecular interactions.

Experimental

All chemicals were purchased from Aldrich and used without further purification. Melting points were determined on a Fisher-Johns melting point apparatus and are uncorrected. ^1H and ^{13}C NMR spectra were recorded on a Varian Unity plus 400 MHz spectrometer in CDCl_3 . Compounds were prepared for infrared spectroscopic (IR) analysis as a mixture in KBr. Elemental analysis was carried out by Atlantic Microlab Inc. Electrospray ionization-trap mass spectrometry (ESI-IT-MS) was carried out on a Bruker Daltonics Esquire 3000 plus. The syntheses and characterizations of 3-(2-amino-4-methylpyrimidin-6-yl)pyridine **1**, 3-(2-amino-4-methoxypyrimidin-6-yl)pyridine **2**, and 1-(2-amino-4-methylpyrimidin-6-yl)-2-(3-methoxypyridin-5-yl)ethyne **3** are reported elsewhere.⁹

2-Amino-5-trimethylsilylethynylpyridine, **4**

2-Amino-5-bromopyridine (5.00 g, 28.9 mmol), trimethylsilylacetylene (3.97 g, 40.4 mmol), copper(I) iodide (0.170 g, 0.890 mmol), triphenylphosphine (0.600 g, 2.29 mmol), bis(triphenylphosphine)palladium(II) dichloride (0.600 g, 0.856 mmol) were added to a round bottom flask. Tetrahydrofuran (65 mL) and triethylamine (65 mL) were added and dinitrogen bubbled through the resultant mixture for 10 minutes. A condenser was attached and the mixture heated at 75°C under a dinitrogen atmosphere. The reaction was monitored by TLC and allowed to cool to room temperature upon completion (48 hours). The solution was then diluted with 100 mL of ethyl acetate, washed with water (3×100 mL) then washed with saturated aqueous sodium chloride (1×100 mL). The organic layer was separated and dried over magnesium sulfate. The solvent was removed on a rotary evaporator and the residue chromatographed on silica with a mixture of hexane/ethyl acetate (10 : 1) as the eluant. **4** was isolated as a light tan solid, which was recrystallized from dichloromethane/hexanes as colorless-opaque plates (4.81 g, 87%). Mp $91\text{--}93^\circ\text{C}$; ^1H NMR (δ_{H} ; 200 MHz, CDCl_3): 8.19 (s, 1H), 7.48 (dd, $J = 8.8$ Hz, $J =$

2.2 Hz, 1H), 6.41 (d, $J = 8.8$ Hz, 1H), 4.52 (s, 2H), 0.23 (s, 9H); ^{13}C NMR (δ_{C} ; 400 MHz, CDCl_3): 157.52, 151.90, 140.73, 109.79, 107.70, 102.74, 94.55, 0.008; IR (KBr): 3452, 3301, 3160, 2156, 1626, 1486, 1390; ESI-IT-MS m/z 192 ($[\mathbf{4} + \text{H}]^+$).

2-Amino-5-ethynylpyridine, **5**

A mixture of 2-amino-5-trimethylsilylethynylpyridine (2.04 g, 10.7 mmol) and potassium carbonate (1.50 g, 10.9 mmol) were stirred in methanol (30 mL) at room temperature for 2 hours. The solution was then diluted with ethyl ether (100 mL) and washed with water (4×100 mL). The solvent was removed on a rotary evaporator and the residue chromatographed on silica with hexanes/ethyl acetate (10 : 1) as the eluant. **5** was isolated as a light brown solid (1.13 g, 92%). Mp $127\text{--}129^\circ\text{C}$; ^1H NMR (δ_{H} ; 400 MHz, CDCl_3): 8.23 (s, 1H), 7.52 (dd, $J = 8.8$ Hz, $J = 2.2$ Hz, 1H), 6.44 (d, $J = 8.8$ Hz, 1H), 4.64 (s, 2H), 3.06 (s, 1H); ^{13}C NMR (δ_{C} ; 200 MHz, CDCl_3)¹⁰: 157.77, 152.11, 140.84, 108.66, 107.79, 81.36; IR (KBr): 3455, 3269, 3155, 2104, 1628, 1500, 1394, 1145, 831; ESI-IT-MS m/z 121 ($[\mathbf{5} + 2\text{H}]^+$).

1-(2-Aminopyrid-5-yl)-2-(pyrid-3-yl)ethyne, **6**

A mixture of 2-amino-5-ethynylpyridine (1.00 g, 8.70 mmol), 3-bromopyridine (1.60 g, 10.12 mmol), copper(I) iodide (0.050 g, 0.262 mmol), triphenylphosphine (0.220 g, 0.840 mmol), bis(triphenylphosphine)palladium(II) dichloride (0.220 g, 0.314 mmol) were added to a round bottom flask. Tetrahydrofuran (30 mL) and triethylamine (30 mL) were added and dinitrogen bubbled through the resultant mixture for 10 minutes. A condenser was attached and the mixture heated at 70°C under a dinitrogen atmosphere. The reaction was monitored by TLC and allowed to cool to room temperature upon completion (36 hours). The solution was then diluted with 100 mL of ethyl acetate, washed with water (3×100 mL) then washed with saturated aqueous sodium chloride (1×100 mL). The organic layer was separated and dried over magnesium sulfate. The solvent was removed on a rotary evaporator and the residue chromatographed on silica with a hexane/ethyl acetate mixture (1 : 1) as the eluant. **6** was isolated as a light brown solid. The product was recrystallized from chloroform producing orange block shaped crystals (1.2 g, 79%). Mp $131\text{--}133^\circ\text{C}$; ^1H NMR (δ_{H} ; 200 MHz, CDCl_3): 8.73

(d, $J = 2.6$ Hz, 1H), 8.52 (dd, $J = 4.9$ Hz, $J = 1.7$ Hz, 1H), 8.28 (d, $J = 2$ Hz, 1H), 7.77 (dt, $J = 8$ Hz, $J = 2$ Hz, 1H), 7.56 (dd, $J = 8.6$ Hz, $J = 2.4$ Hz, 1H), 7.27 (m, 1H), 6.49 (dd, $J = 8.4$ Hz, $J = 0.8$ Hz, 1H), 4.77 (s, 1H); ^{13}C NMR (δ_{C} ; 200 MHz, CDCl_3): 157.79, 152.02, 151.50, 148.29, 140.39, 138.09, 122.96, 120.60, 109.08, 107.96, 90.37, 86.53; IR (KBr): 3318, 3140, 2213, 1602, 1508, 1398; ESI-IT-MS m/z 197 ($[\text{6} + \text{H}]^+$).

Tetrakis(μ -acetato- O,O')-bis(3-(2-amino-4-methylpyrimidin-6-yl)pyridine)-dicopper(II), 7

3-(2-Amino-4-methylpyrimidin-6-yl)pyridine (9 mg, 0.05 mmol) and copper(II) acetate (10 mg, 0.05 mmol) were added to a screw cap vial along with a methanol/acetonitrile mixture (2 : 1 mL). The mixture was heated gently until a clear homogeneous solution resulted. Without solvent evaporation, green block-shaped crystals were collected after 1 day. Mp 210–212 °C. Anal. Calcd. for $\text{C}_{28}\text{H}_{32}\text{N}_8\text{O}_8\text{Cu}_2$: C, 45.77; H, 4.39; N, 15.26. Found: C, 45.72; H, 4.46; N, 15.09%.

Tetrakis(μ -2-fluorobenzoato- O,O')-bis(3-(2-amino-4-methylpyrimidin-6-yl)pyridine)-dicopper(II), 8

3-(2-Amino-4-methylpyrimidin-6-yl)pyridine (9 mg, 0.05 mmol) and copper(II) 2-fluorobenzoate (16 mg, 0.02 mmol) were added to a screw cap vial along with a mixture of methanol/acetonitrile (1 : 5 mL). The mixture was heated gently until a clear homogeneous solution resulted. Without solvent evaporation, green plate-shaped crystals were collected after 1 day. Mp 224–226 °C. Anal. Calcd. for $\text{C}_{48}\text{H}_{36}\text{N}_8\text{O}_8\text{F}_4\text{Cu}_2 \cdot \text{H}_2\text{O}$: C, 53.75; H, 3.57; N, 10.45. Found: C, 53.69; H, 3.30; N, 10.45%.

Tetrakis(μ -acetato- O,O')-bis(3-(2-amino-4-methoxypyrimidin-6-yl)pyridine)-dicopper(II), 9

3-(2-Amino-4-methoxypyrimidin-6-yl)pyridine (10 mg, 0.05 mmol) and copper(II) acetate (10 mg, 0.05 mmol) were added to a screw cap vial along with a methanol/acetonitrile mixture (2 : 1 mL). The mixture was heated gently until a clear homogeneous solution resulted. Without solvent evaporation, green block-shaped crystals were harvested after 1 day. Mp 212 °C (decomp.). Anal. Calcd. for $\text{C}_{28}\text{H}_{32}\text{N}_8\text{O}_{10}\text{Cu}_2$: C, 43.86; H, 4.21; N, 14.62. Found: C, 43.62; H, 4.19; N, 14.57%.

Tetrakis(μ -2-fluorobenzoato- O,O')-bis(3-(2-amino-4-methoxypyrimidin-6-yl)pyridine)-dicopper(II), 10

3-(2-Amino-4-methoxypyrimidin-6-yl)pyridine (9 mg, 0.05 mmol) and copper(II) 2-fluorobenzoate (17 mg, 0.03 mmol) were added to a screw cap vial along with a mixture of methanol/acetonitrile (1 : 5 mL). The mixture was heated gently until a clear homogeneous solution resulted. Without solvent evaporation, green plate-shaped crystals were collected after 1 day. Mp 224–226 °C. Anal. Calcd. for $\text{C}_{48}\text{H}_{36}\text{N}_8\text{O}_{10}\text{F}_4\text{Cu}_2$: C, 53.03; H, 3.34; N, 10.31. Found: C, 52.92; H, 3.14; N, 10.22%.

Tetrakis(μ -acetato- O,O')-bis(1-(2-amino-4-methylpyrimidin-6-yl)-2-(3-methoxypyridin-5-yl)ethyne)-dicopper(II), 11

1-(2-Amino-4-methylpyrimidin-6-yl)-2-(3-methoxypyridin-5-yl)ethyne (10 mg, 0.04 mmol) and copper(II) acetate (17 mg,

0.08 mmol) were added to a screw cap vial along with a 1 : 1 : 1 mixture of ethanol/acetonitrile/nitromethane. The mixture was heated gently until a clear homogeneous solution resulted. Without solvent evaporation, green block-shaped crystals were collected after 2 days. Mp 160 °C (decomp.). Anal. Calcd. for $\text{C}_{34}\text{H}_{36}\text{N}_8\text{O}_{10}\text{Cu}_2$: C, 48.45; H, 4.31; N, 13.30. Found: C, 48.11; H, 4.28; N, 13.28%.

Tetrakis(μ -2-fluorobenzoato- O,O')-bis(1-(2-aminopyrid-5-yl)-2-(pyrid-3-yl)ethyne)-dicopper(II), 12

1-(2-Aminopyridin-5-yl)-2-(pyridin-3-yl)ethyne (11 mg, 0.06 mmol) and copper(II) 2-fluorobenzoate (19 mg, 0.03 mmol) were added to a screw cap vial along with a mixture of methanol/acetonitrile (3 : 5 mL). The mixture was heated gently until a clear homogeneous solution resulted. Without solvent evaporation, green plate-shaped crystals were collected after 1 day. Mp 255 °C (decomp.). Anal. Calcd. for $\text{C}_{40}\text{H}_{25}\text{N}_3\text{O}_8\text{F}_4\text{Cu}_2$: C, 54.73; H, 2.87; N, 4.79. Found: C, 54.65; H, 2.89; N, 4.96%.

Tetrakis(μ -acetato- O,O')-bis(1-(2-aminopyrid-5-yl)-2-(pyrid-3-yl)ethyne)-dicopper(II), 13

1-(2-Aminopyrid-5-yl)-2-(pyridin-3-yl)ethyne (13 mg, 0.07 mmol) and copper(II) acetate (26 mg, 0.13 mmol) were added to a screw cap vial along with a mixture of methanol/acetonitrile (3 : 5 mL). The mixture was heated gently until a clear homogeneous solution resulted. Without solvent evaporation, green block-shaped crystals were collected after 1 day. Mp 210 °C (decomp.). Anal. Calcd. for $\text{C}_{20}\text{H}_{21}\text{N}_3\text{O}_8\text{Cu}_2$: C, 43.09; H, 3.80; N, 7.54. Found: C, 42.92; H, 3.77; N, 7.54%.

X-Ray crystallography

X-Ray data were collected on a Bruker SMART CCD diffractometer (7–13)¹¹ using Mo- $K\alpha$ radiation. Data were collected using SMART.¹² Initial cell constants were found by small widely separated “matrix” runs. An entire hemisphere of reciprocal space was collected. Scan speed and scan width were chosen based on scattering power and peak rocking curves. All datasets were collected at low temperature.

Unit cell constants and orientation matrix were improved by least-squares refinement of reflections thresholded from the entire dataset. Integration was performed with SAINT,¹³ using this improved unit cell as a starting point. Precise unit cell constants were calculated in SAINT from the final merged dataset. Lorentz and polarization corrections were applied, and data were corrected for absorption.

Data were reduced with SHELXTL.¹⁴ The structures were solved in all cases by direct methods without incident. In general, hydrogens were assigned to idealized positions and were allowed to ride. Where possible, the coordinates of hydrogen-bonding hydrogens were allowed to refine. Heavy atoms were refined with anisotropic thermal parameters. Crystallographic data are given in Table 1, hydrogen bond geometries in Table 2 and thermal ellipsoids and labeling schemes are shown in Fig. 1, 3, 6, 8, 10, 12.

CCDC reference numbers 278015–278021.

For crystallographic data in CIF or other electronic format see DOI: 10.1039/b513765a

Table 1 Crystallographic data for compounds 7–13

	7	8	9	10	11	12	13
Systematic name	Tetrakis(μ -acetato- <i>O,O'</i>)-bis[3-(2-amino-6-methylpyrimidin-6-yl)pyridine] Cu(II)	Tetrakis(μ -acetato- <i>O,O'</i>)-bis[3-(2-amino-6-methylpyrimidin-6-yl)pyridine] Cu(II)	Tetrakis(μ -acetato- <i>O,O'</i>)-bis[3-(2-amino-6-methoxy-pyrimidin-6-yl)pyridine] Cu(II)	Tetrakis(μ -2-fluorobenzoato- <i>O,O'</i>)-bis[3-(2-amino-4-methoxy-pyrimidin-6-yl)pyridine] Cu(II)	Tetrakis(μ -acetato- <i>O,O'</i>)-bis[1-(2-amino-4-methylpyrimidin-6-yl)-2-(3-methoxy-pyridin-5-yl)ethyne] Cu(II)	Tetrakis(μ -2-fluorobenzoato- <i>O,O'</i>)-bis[1-(2-amino-pyridin-3-yl)ethyne] Cu(II)	Tetrakis(μ -acetato- <i>O,O'</i>)-bis[1-(2-aminopyridin-5-yl)-2-(pyridin-3-yl)ethyne] Cu(II)
Formula moiety	(C ₁₄ H ₈ O ₄) ₂ (C ₁₀ H ₁₀ N ₄) ₂ -Cu ₂	(C ₁₄ H ₈ F ₂ O ₄) ₂ -(C ₁₀ H ₁₀ N ₄) ₂ Cu ₂	(C ₁₄ H ₈ O ₄) ₂ -(C ₁₀ H ₁₀ N ₄ O ₂) ₂ Cu ₂	(C ₁₄ H ₈ F ₂ O ₄) ₂ -(C ₁₀ H ₁₀ N ₄ O ₂) ₂ Cu ₂	(C ₁₄ H ₈ O ₄) ₂ -(C ₁₄ H ₁₂ N ₄ O ₂) ₂ Cu ₂	(C ₁₄ H ₈ F ₂ O ₄) ₂ -(C ₁₂ H ₆ N ₄) ₂ Cu ₂	(C ₁₄ H ₈ O ₄) ₂ (C ₁₂ H ₆ N ₄) ₂ -Cu ₂
Empirical formula	C ₂₈ H ₃₂ Cu ₂ N ₈ O ₈	C ₄₈ H ₃₆ Cu ₂ F ₄ N ₈ O ₈	C ₂₈ H ₃₂ Cu ₂ N ₈ O ₁₀	C ₄₈ H ₃₆ Cu ₂ F ₄ N ₈ O ₁₀	C ₃₄ H ₃₆ Cu ₂ N ₈ O ₁₀	C ₄₀ H ₂₅ Cu ₂ F ₄ N ₆ O ₈	C ₂₀ H ₂₁ Cu ₂ N ₃ O ₈
Molecular weight	735.70	1055.93	767.70	1087.93	903.67	878.71	558.48
Color, habit	Green, prism	Green, prism	Green, prism	Green, prism	Green, prism	Green, plate	Green, block
Space group, Z	P2(1)/c, 2	P2(1)/c, 4	P1, 1	P1, 1	P1, 1	P2(1)/c, 2	P1, 1
<i>a</i> /Å	8.0282(5)	21.3553(18)	8.2800(6)	10.1310(9)	7.6304(13)	9.3471(9)	8.1368(11)
<i>b</i> /Å	10.6399(7)	17.9389(15)	9.3983(6)	10.5499(8)	11.3870(19)	15.5850(15)	8.3062(11)
<i>c</i> /Å	18.9041(13)	11.4887(9)	11.2233(7)	12.2936(9)	12.341(2)	12.9025(11)	8.7490(12)
<i>a</i> /°	90	90	71.144(4)	64.853(5)	76.216(3)	90	86.244(3)
<i>b</i> /°	99.3600(10)	90.742(5)	81.585(4)	86.149(5)	84.191(3)	104.714(7)	80.480(3)
<i>γ</i> /°	90	90	79.240(4)	67.896(4)	79.459(3)	90	80.539(3)
<i>V</i> /Å ³	1593.27(18)	4400.8(6)	808.49(9)	1095.24(15)	1021.9(3)	1817.9(3)	574.79(13)
ρ /g cm ⁻³	1.534	1.594	1.577	1.649	1.468	1.605 g/cm ³	1.613
<i>T</i> /K	173(2)	173(2)	173(2)	173(2)	100(2)	173(2)	100(2)
X-Ray wavelength	0.71073	0.71073	0.71073	0.71073	0.71073	0.71073	0.71073
μ /mm ⁻¹	1.396	1.050	1.383	1.061	1.108	1.250	1.900
Reflections collected	17891	31431	6060	7872	9372	12614	11035
independent	4630	9998	3638	4793	5732	4188	11035
observed	4270	6283	3063	3808	4969	2321	9049
Threshold expression	>2 σ (<i>I</i>)	>2 σ (<i>I</i>)	>2 σ (<i>I</i>)	>2 σ (<i>I</i>)	>2 σ (<i>I</i>)	>2 σ (<i>I</i>)	>2 σ (<i>I</i>)
<i>R</i> ₁ (observed)	0.0280	0.0470	0.0376	0.0580	0.0467	0.0598	0.0553
<i>wR</i> ₂ (all)	0.0825	0.1240	0.0999	0.1635	0.1352	0.1457	0.1398
<i>T</i> -min	0.781	No absorption cor.	0.825	No absorption cor.	0.796	No absorption cor.	No absorption cor.
<i>R</i> merge	2.24%	7.34%	2.37%	7.85%	1.69%	13.68	N/A (twinned)

Table 2 Selected hydrogen bond lengths (Å) and angles (°) for compounds 7–13

	D–H...A	D–H	H...A	D...A	<(DHA)
7	N(12)–H(12A)...N(11)#2 ^a	0.87(2)	2.17(2)	3.0434(17)	175(2)
	N(12)–H(12B)...O(42)#3	0.89(2)	2.10(2)	2.9748(16)	170.5(19)
8	N(22)–H(22A)...N(63)#2 ^b	0.93(4)	2.31(4)	3.241(4)	174(3)
	N(22)–H(22B)...O(78)	0.95(4)	2.26(4)	3.206(4)	173(3)
	N(62)–H(62A)...N(21)#2	0.73(4)	2.27(4)	3.001(4)	171(4)
9	N(62)–H(62B)...O(48)#3	0.83(4)	2.27(4)	3.055(4)	159(3)
	N(12)–H(12A)...N(11)#2 ^c	0.95(3)	2.24(3)	3.177(3)	171(2)
	N(12)–H(12B)...O(41)#2	0.91(3)	2.29(3)	3.185(3)	170(3)
10	N(22)–H(22A)...N(23)#2 ^d	0.88	2.52	3.253(5)	141.2
11	N(12)–H(12A)...O(42)#2 ^e	0.82(4)	2.22(4)	2.982(3)	155(3)
	N(12)–H(12B)...N(11)#3	0.72(3)	2.34(4)	3.061(3)	173(3)
12	N(12)–H(12B)...O(38)#3 ^f	0.88	2.43	3.295(8)	168.3
13	N(16)–H(16B)...O(31)#3 ^g	0.88	2.32	3.078(3)	144.5

^a #2 $-x, -y + 1, -z + 1$. #3 $-x + 1, y - 1/2, -z + 1/2$. ^b #2 $-x + 1, -y + 1, -z + 1$. #3 $x - 1, y, z$. ^c #2 $-x + 1, -y, -z + 1$. ^d #2 $-x + 1, -y + 1, -z$. ^e #2 $x, y - 1, z + 1$. #3 $-x, -y, -z + 2$. ^f #3 $x + 1, y, z$. ^g #3 $-x + 1, -y + 1, -z + 1$.

Results

Ligand **6** was produced in good yields by reacting 2-amino-5-ethynylpyridine with 3-bromopyridine under an inert atmosphere. 2-Amino-5-ethynylpyridine was synthesized in excellent yields by means of Pd-catalyzed Sonogashira coupling conditions¹⁵ of 2-amino-5-bromopyridine and trimethylsilylacetylene followed by base-promoted deprotection, Scheme 3.

The complex-ion in the crystal structure of **7** is composed of two pyridine-pyrimidine (py-pym) ligands **1** bound at the axial positions of the dicopper tetraacetate complex, Fig. 1. The symmetry-related Cu(II) ion displays a square-pyramidal coordination geometry with Cu–N distances of 2.1743(11) Å. The complex ions are assembled into infinite chains through self-complementary N–H...N hydrogen bonds, between the *syn*-amino proton and a pyrimidine nitrogen atom. Neighboring chains are subsequently organized into a 2-D sheet *via* N–H...O hydrogen bonds between the *anti*-amino proton and an acetate oxygen atom from an adjacent strand, Fig. 2(a) and (b).

The crystal structure of **8** contains two crystallographically unique Cu(II)-complexes, Fig. 3. Within each complex the copper ions are arranged in the familiar “paddlewheel” motif in which two copper ions are bridged by four acetate groups, thus leaving two axial sites for further coordination. The two py-pym ligands **1** are coordinated axially through the nitrogen atom of the pyridyl moiety to the Cu(II) ions, each with a square-pyramidal geometry with Cu–N distances of 2.145(3) and 2.149(2) Å respectively. The two unique complexes are connected in a zig-zag manner through

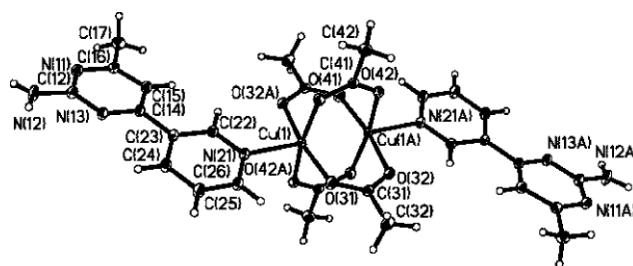
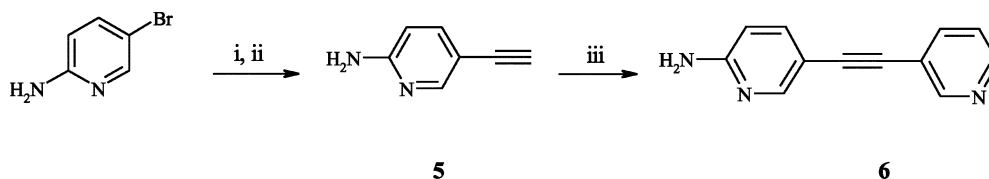


Fig. 1 Labeled thermal ellipsoids of **7** (50% probability level).

self-complementary N–H...N hydrogen bonds, produced from the *syn*-amino proton and a pyrimidine nitrogen atom, Fig. 4.

This feature is then extended into a 2-D sheet through N–H...O hydrogen bonds from the *anti*-amino proton to an adjacent acetate oxygen atom from an adjacent strand, Fig. 5.

The complex-ion in the crystal structure of **9** contains two py-pym ligands **2** bound axially through their pyridyl nitrogen atoms to the dicopper tetraacetate dimer affording a five-coordinate square-pyramidal geometry around each Cu(II) ion with a Cu–N distance of 2.169(2) Å, Fig. 6. Discrete one-dimensional chains are formed from self-complementary N–H...N hydrogen bonds between the *syn*-amino proton and a pyrimidine nitrogen atom, whilst the *anti*-amino proton hydrogen bonds with a neighboring acetate oxygen atom through N–H...O interactions, Fig. 7. The second nitrogen atom of the pyrimidine ring is blocked by the adjacent methoxy substituent and does not act as a hydrogen-bond acceptor.



(i) Me_3SiCCH , $\text{Cl}_2\text{Pd}(\text{PPh}_3)_2$, PPh_3 , NEt_3 , thf ; (ii) K_2CO_3 , MeOH ;
(iii) 3-bromopyridine, $\text{Cl}_2\text{Pd}(\text{PPh}_3)_2$, PPh_3 , NEt_3 , thf .

Scheme 3 Synthesis of **5** and **6**.

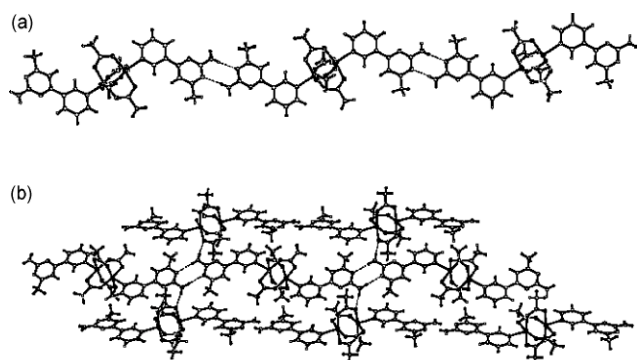


Fig. 2 (a) One-dimensional strand in **7** formed by self-complementary N-H...N hydrogen bonds (top); (b) two-dimensional sheet produced in **7** from a combination of N-H...N and N-H...O hydrogen bonds (bottom).

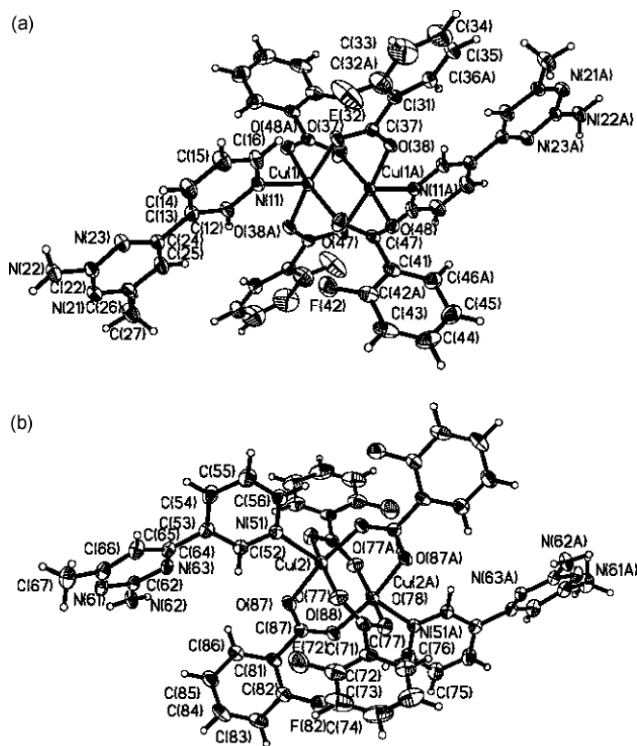


Fig. 3 Labeled thermal ellipsoids of the two unique complex ions (a and b) in **8** (50% probability level).

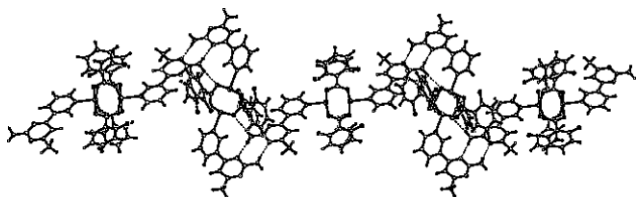


Fig. 4 1-D zig-zag chain in **8** produced through self-complementary N-H...N hydrogen bonds.

The complex ion in the crystal structure of **10** contains two py-pym ligands **2** bound axially *via* the pyridyl nitrogen atoms to the “paddlewheel” copper dimer unit, furnishing each Cu(II) ion with a square-pyramidal coordination geometry with Cu–N

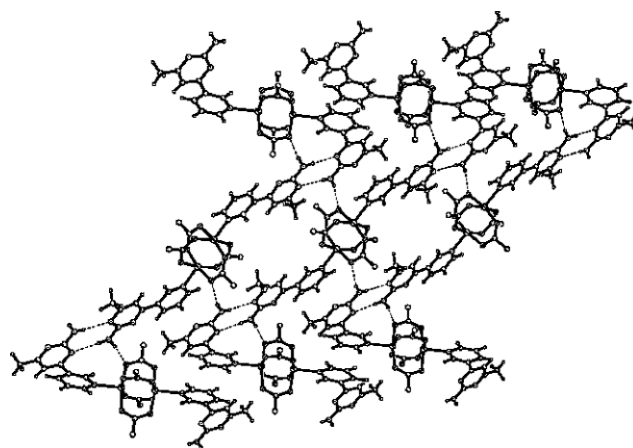


Fig. 5 Extended network of **8** through a series of N-H...N and N-H...O hydrogen bonds (the fluoro-phenyl rings have been omitted for clarity).

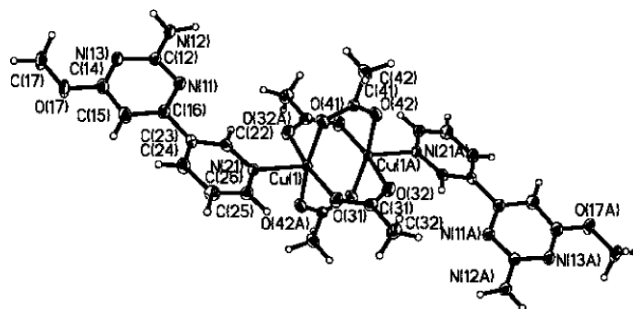


Fig. 6 Labeled thermal ellipsoids of **9** (50% probability level).

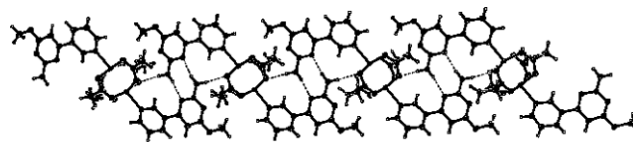


Fig. 7 Infinite chain in **9** formed from Cu(II)-py coordination bonds and self-complementary N-H...N and heteromeric N-H...O hydrogen bonds.

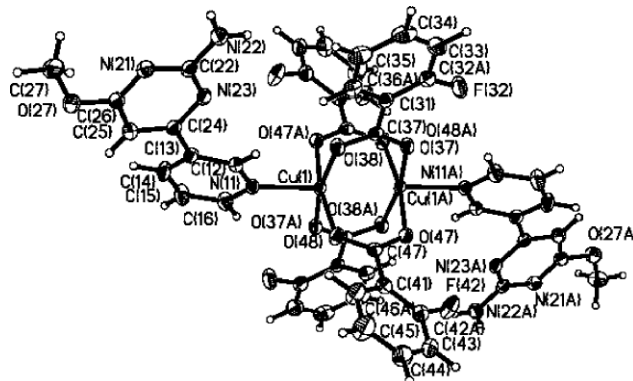


Fig. 8 Labeled thermal ellipsoids of **10** (50% probability level).

distances of 2.149(3) Å, Fig. 8. Similar to structure **9**, discrete 1-D chains are produced from self-complementary N-H...N hydrogen bonds from the *syn*-amino proton to a pyrimidine nitrogen atom, and N-H...O interactions from the *anti*-amino

proton to an acetate oxygen atom of a neighboring strand, Fig. 9. Additional stabilization of the network is provided by π – π stacking between the fluoro-substituted phenyl rings and the amino-pyrimidine rings with distances as short as 3.28 Å.

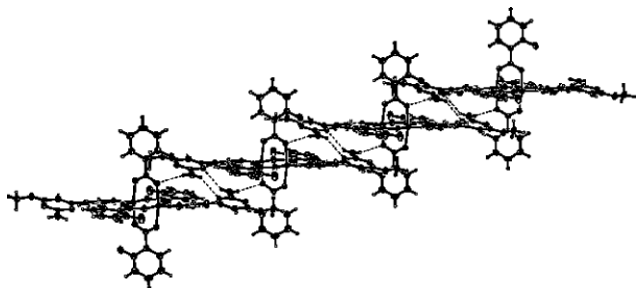


Fig. 9 1-D stair-step architecture stabilized by a combination of hydrogen bonds and π – π -stacking in **10**.

The crystal structure of **11** contains two py-pym ligands **3** bound in the axial positions of the two Cu(II) ions contained within the tetraacetate “paddlewheel” unit, creating a square-pyramidal coordination geometry around each copper ion with Cu–N distances of 2.181(18) Å, Fig. 10. Discrete infinite 1-D chains are produced from self-complementary N–H···N hydrogen bonds between the *syn*-amino proton and a pyrimidine nitrogen atom, Fig. 11. Neighboring chains are subsequently organized into a 2-D sheet *via* N–H···O hydrogen bonds between the *anti*-amino proton and an acetate oxygen atom from an adjacent strand, similar to what was observed in the structure of **7**.

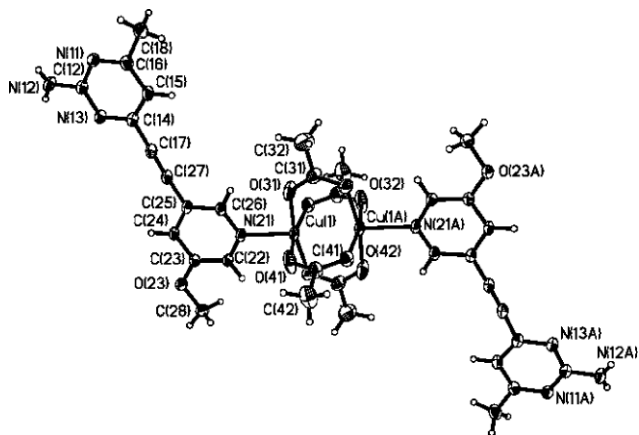


Fig. 10 Labeled thermal ellipsoids of **11** (50% probability level).

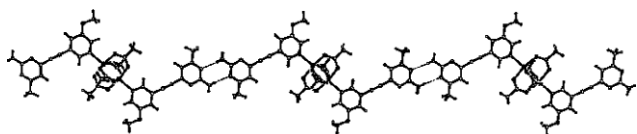


Fig. 11 1-D strand in **11** formed through self-complementary amino-pyrimidine N–H···N hydrogen bonds.

In the crystal structures of **12** and **13** there are two pyridine-pyridine (py-py) ligands **6** bound axially, through the pyridyl nitrogen atoms to the “paddlewheel” copper dimer unit, creating a square-pyramidal coordination geometry with Cu–N distances

of 2.162(3) and 2.198 (14) Å respectively. In both structures the py-py ligand **6** is essentially located on an inversion center, with NH₂ and H randomly disordered with 50% occupancy. Thus, the complex ions are shown with both ends of the ligand containing an amino group, Fig. 12. Although the ligand contains a potential self-complementary N–H···N hydrogen bonding moiety, no hydrogen bonds are formed between adjacent ligands. Instead, both pyridyl moieties coordinate to two different “paddlewheel” units which, in effect, creates 1-D coordination polymers within the lattice of both **12** and **13**.

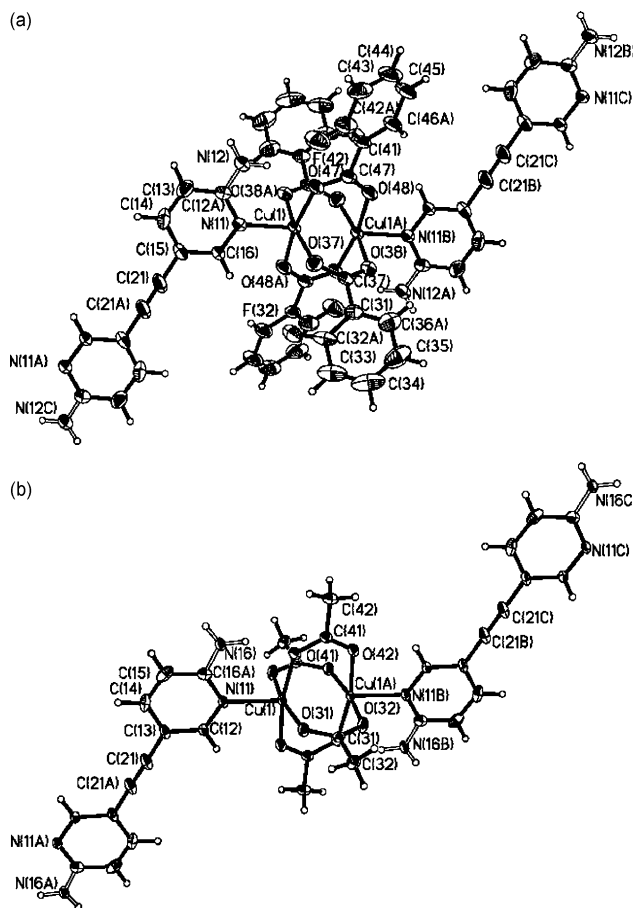


Fig. 12 Labeled thermal ellipsoids of **12** (a) and **13** (b) at 50% probability level.

Discussion

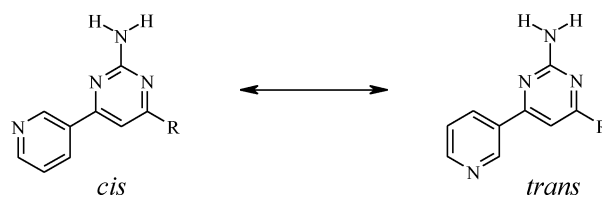
In order to direct the assembly of complex ions into extended inorganic–organic networks of specific (and pre-determined) dimensionality or geometry, it is necessary to achieve and maintain control over both the immediate coordination environment around the central metal ion, and over the way in which neighboring complex ions recognize and interact with each other. By incorporating the metal ion within an overall electrically neutral building block, the need for potentially disruptive counterions has been eliminated. In this study, we opted to start with tetrakis(μ -carboxylato-*O,O'*)-dicopper(II) complexes as these architectures are neutral and they offer two available binding sites (axial positions) that are organized in such a way as to produce, essentially, a linear metal-containing building block. In all seven

crystal structures obtained in this effort, the desired coordination environment around each copper (II) ion was achieved resulting in rigid neutral dicopper(II) tetracarboxylate complexes. The next phase in the supramolecular synthesis requires some means for aligning and connecting these complex ions in such a way that the inherent geometry of the metal complex is propagated into extended Cu-containing networks. We therefore examined the ability of four different bifunctional ligands to act as supramolecular reagents for the construction of 1-D motifs. All four ligands are potentially capable of forming the desired architectures by virtue of having a pyridyl moiety as a binding site for the metal, coupled with an amino-pyrimidine or amino-pyridine moiety proficient in forming self-complementary N–H...N/N...H–N interactions.

In all seven structures **7–13**, the pyridyl moiety provides a robust and reliable binding site for attaching the supramolecular bifunctional ligand to the open, axial coordination sites on the Cu(II) ion. For the supramolecular chemistry, three of the ligands utilize an aminopyrimidine moiety, whereas one ligand, **6**, relies on an amino-pyridine functionality. For the two structures, **12** and **13**, where the latter ligand was employed, the desired intermolecular interactions failed to materialize. Surprisingly, the disordered bipyridine-type ligands acted as ditopic linkers between adjacent Cu(II)-ions resulting in 1-D coordination polymers. The reason for the failure of **6** to act in the desired manner is not obvious, but it is possible that the pyridyl moiety, which is an integral part of the hydrogen-bonding functionality, is simply too good a ligand to give up a Cu(II) ion in exchange for acting as an acceptor in an N–H...N hydrogen bond. This interpretation is supported by the fact that when a pyridyl moiety is replaced with a less effective ligand, a pyrimidine heterocycle, a dimeric hydrogen-bond motif is favored over a pyrimidine–Cu, ligand–metal, interaction.

Each time a bifunctional ligand with a pyrimidine component was employed (all five of the structures), neighboring ligands were connected *via* a dimeric N–H...N motif. The exact directional and structural consequence of this interaction is, however, complicated by the fact that the 2-aminopyrimidine moieties, employed in this study, are asymmetric about the C1–C4 vector, Scheme 2. Consequently, each bifunctional ligand, **1–3**, has two different ways of producing a self-complementary N–H...N/N...H–N motif. If the hydrogen bonds between adjacent 2-aminopyrimidine moieties serve to maximize the through-space separation between metal ions, Scheme 4a, the result is a diverging assembly, whereas if the N–H...N/N...H–N synthon brings the complex ions closer together, Scheme 4b, the assembly is converging.

Another variable that needs to be taken into consideration is the fact that the pyridyl moiety and the 2-amino substituent can be arranged either *cis* or *trans* with respect to each other, Scheme 5.



Scheme 5 Possible *cis* or *trans* isomers based on the arrangement of the pyridine nitrogen atom and the 2-amino substituent.

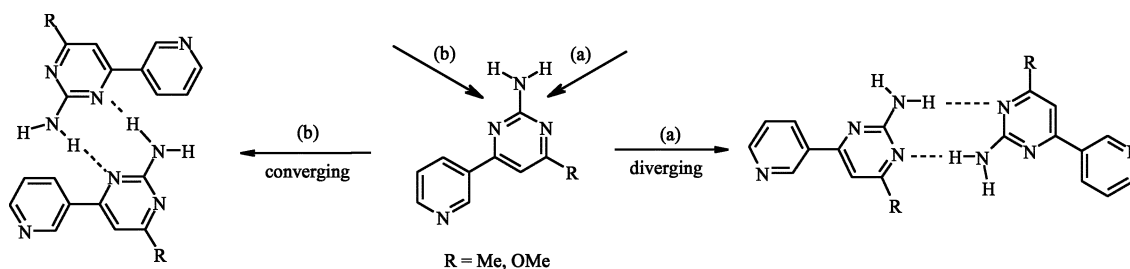
Steric considerations dictate that only one of the two arrangements is possible in any given structure but, from a supramolecular synthetic viewpoint, it would be of interest to establish whether or not a suitable molecular substitution can provide a tool for guiding this particular assembly process in a rational manner.

The two crystal structures **9** and **10** display the same converging motifs, Scheme 4b, due to the fact that the OMe substituent blocks the adjacent cyclic nitrogen atom, and thus prevents it from participating as an acceptor in a self-complementary N–H...N/N...H–N motif.

The two crystal structures **7** and **11** possess diverging motifs, Scheme 4a, and in both cases the 2-amino moiety is *trans* to the pyridyl nitrogen. The methyl substituent present on the pyrimidine ring does not seem large enough to control the relative interplanar orientation in the bifunctional ligands and it is not clear if a specific interaction is responsible for the observed orientation. It is likely to be a combination of factors that are responsible for the details of the direction of the N–H...N dimer.

The crystal structure of **8** provides a good example of the difficulties that can be encountered when trying to establish clear structural patterns and/or intermolecular preferences. In this structure there are two crystallographically unique metal-containing building blocks: one with a *cis*, and one with a *trans* orientation of the 2-amino functionality with respect to the pyridyl moiety. The former ligand gives rise to a converging assembly, whereas the latter produces a divergent motif.

The principle supramolecular target for this study, Cu(II)-containing 1-D assemblies was realized in a reasonable supramolecular yield using a combination of new bifunctional ligands and the well-known μ -*O,O'* coordinating mode of the carboxylate functionality. In each case, we successfully controlled the coordination geometry around the often unpredictable Cu(II) ion. We were quite successful, five of seven structures, in connecting neighboring complex-ions into infinite 1-D chains using ligand–ligand N–H...N/N...H–N hydrogen bonds. The exact nature of the assembly, convergent or divergent, is determined by the relative orientation of the two aromatic components of our bifunctional



Scheme 4 Pictorial description of converging or diverging structural motifs.

ligands, which, in turn, can be represented by the rather soft potential energy curve typically associated with aryl–aryl torsion angles.

In a sense, our supramolecular success mirrors quite closely the relative strengths of the interactions that are responsible for the different recognition and binding events that take place in the course of these reactions: metal–ligand (100%), hydrogen-bonds (71%) and van der Waals forces (50%).

We are beginning to gain a better understanding of how to design supramolecular ligands and synthetic strategies in such a way as to minimize unwanted structural interference. However, in order to make more, and more rapid, progress we will require further systematic studies that clearly represent the overall supramolecular outcome, success and failure, with respect to clearly delineated assembly strategies.

Acknowledgements

Financial support from NSF (CHE-0316479) and Kansas State University is gratefully acknowledged. We also thank Takeo Iwamoto for the ESI-IT-MS data collections.

References and notes

- (a) K.-W. Chi, C. Addicott, A. M. Arif and P. J. Stang, *J. Am. Chem. Soc.*, 2004, **126**, 16569; (b) B. Chatterjee, J. C. Noveron, M. J. E. Resendiz, J. Liu, T. Yamamoto, D. Parker, M. Cinke, C. V. Nguyen, A. M. Arif and P. J. Stang, *J. Am. Chem. Soc.*, 2004, **126**, 10645; (c) K. Nakabayashi, M. Kawano, M. Yoshizawa, S. Ohkoshi and M. Fujita, *J. Am. Chem. Soc.*, 2004, **126**, 16694.
- (a) M. Yoshizawa, S. Miyagi, M. Kawano, K. Ishiguro and M. Fujita, *J. Am. Chem. Soc.*, 2004, **126**, 9172; (b) M. Fujita, M. Tominaga, A. Hori and B. Therrien, *Acc. Chem. Res.*, 2005, **38**, 369; (c) M. Yoshizawa, Y. Takeyama, T. Okano and M. Fujita, *J. Am. Chem. Soc.*, 2003, **125**, 3243; (d) J. L. C. Rowsell and O. M. Yaghi, *Microporous Mesoporous Mater.*, 2004, **73**, 3; (e) J. L. C. Rowsell, A. R. Millward, K. S. Park and O. M. Yaghi, *J. Am. Chem. Soc.*, 2004, **126**, 5666; (f) J. L. Atwood, L. J. Barbour, S. J. Dalgarno, M. J. Hardie, C. L. Raston and H. R. Webb, *J. Am. Chem. Soc.*, 2004, **126**, 13170.
- (a) R. J. Hill, D.-L. Long, N. R. Champness, P. Hubberstey and M. Schroder, *Acc. Chem. Res.*, 2005, **38**, 335; (b) K. Campbell, C. J. Kuehl, M. J. Ferguson, P. J. Stang and R. R. Tykwinski, *J. Am. Chem. Soc.*, 2002, **124**, 7266; (c) D. Braga, S. L. Gialfreda, F. Grepioni and M. Polito, *CrystEngComm*, 2004, **6**, 458–462; (d) J. F. Berry, F. A. Cotton, C. S. Fewox, T. Lu, C. A. Murillo and X. Wang, *Dalton Trans.*, 2004, **15**, 2297; (e) G. J. McManus, Z. Wang and M. J. Zaworotko, *Cryst. Growth Des.*, 2004, **4**, 11; (f) D. Braga, L. Brammer and N. R. Champness, *CrystEngComm*, 2005, **7**, 1; (g) N. Schultheiss, C. L. Barnes and E. Bosch, *Cryst. Growth Des.*, 2003, **3**, 573; (h) M. Oh, C. L. Stern and C. A. Mirkin, *Inorg. Chem.*, 2005, **44**, 2647.
- (a) *Supramolecular Assembly via Hydrogen Bonds II. Structure and Bonding*, ed. D. M. P. Mingos, Springer-Verlag, Berlin, Heidelberg, New York, 2004; (b) G. R. Desiraju, *Acc. Chem. Res.*, 1996, **29**, 441; (c) C. B. Aakeroy, A. M. Beatty and B. A. Helfrich, *J. Am. Chem. Soc.*, 2002, **124**, 14425; (d) F. M. Raymo, M. D. Bartberger, K. N. Houk and J. F. Stoddart, *J. Am. Chem. Soc.*, 2001, **123**, 9264; (e) J.-H. Fournier, T. Maris, J. D. Wuest, W. Guo and E. Galoppini, *J. Am. Chem. Soc.*, 2003, **125**, 1002; (f) D. Braga, M. Polito, D. D'Addario and F. Grepioni, *Cryst. Growth Des.*, 2004, **4**, 1109.
- (a) O. Ohmori, M. Kawano and M. Fujita, *CrystEngComm*, 2005, **7**, 255; (b) A. Sundararaman, L. N. Zakharov, A. L. Rheingold and F. Jaekle, *Chem. Commun.*, 2005, **13**, 1708; (c) E. V. Garcia-Baez, F. J. Martinez-Martinez, H. Hoepfl and I. I. Padilla-Martinez, *Cryst. Growth Des.*, 2003, **3**, 35; (d) A. J. Blake, N. R. Champness, A. N. Khlobystov, D. A. Lemenovskii, W.-S. Li and M. Schroder, *Chem. Commun.*, 1997, **15**, 1339; (e) A. B. Oren, M. D. Curtis and J. W. Kampf, *Chem. Mater.*, 2000, **12**, 1519.
- (a) C. B. Aakeroy, A. M. Beatty and K. R. Lorimer, *J. Chem. Soc., Dalton Trans.*, 2000, **21**, 3869; (b) C. B. Aakeroy, A. M. Beatty, D. S. Leinen and K. R. Lorimer, *Chem. Commun.*, 2000, **11**, 935; (c) C. B. Aakeroy, A. M. Beatty, J. Desper, M. O'Shea and J. Valdés-Martínez, *Dalton Trans.*, 2003, **20**, 3956; (d) D. Bose, J. Banerjee, S. H. Rahaman, G. Mostafa, H.-K. Fun, R. D. Bailey Walsh, M. J. Zaworotko and B. K. Ghosh, *Polyhedron*, 2004, **23**, 2045; (e) T. J. Burchell, D. J. Eisler and R. J. Puddephatt, *Inorg. Chem.*, 2004, **43**, 5550.
- (a) D. W. Thompson, *On Growth and Form*, Cambridge University Press, Cambridge, 1942; (b) S. J. Mann, *J. Chem. Soc., Dalton Trans.*, 1997, **21**, 3953; (c) M. Li and S. Mann, *J. Mater. Chem.*, 2004, **14**, 2260; (d) S. Mann, *Chem. Commun.*, 2004, **1**, 1.
- (a) P. Wu, M. Bhamidipati, M. Coles and D. V. G. L. N. Roa, *Chem. Phys. Lett.*, 2004, **400**, 506; (b) B. J. Kooi, J. Th and M. De Hosson, *J. Appl. Phys.*, 2004, **95**, 4714; (c) H. Okumura, D. J. Twisselmann, R. D. McMichael, M. Q. Huang, Y. N. Hsu, D. E. Laughlin and M. E. McHenry, *J. Appl. Phys.*, 2003, **93**, 6528.
- C. B. Aakeroy, N. Schultheiss and J. Desper, *Inorg. Chem.*, 2005, **44**, 4983.
- A single sp-carbon is missing from the ^{13}C NMR spectra.
- Compound **7**: Data were collected on a SMART APEX at 100 K. The copper complex sits on a crystallographic inversion center. Coordinates for the amine hydrogens, H12A and H12B, were allowed to refine. Compound **8**: Data were collected on a SMART 1000 at 100 K. The lattice contains two independent copper complexes, each sitting on a crystallographic inversion center. Two of the four 2-fluorobenzoates existed in two nearly superimposable rotamers, differing in the relative placement of the fluorine substituent. Coordinates for the amine hydrogens, H22A, H22B, H62A, and H62B, were allowed to refine. Compound **9**: Data were collected on a SMART 1000 at 100 K. The copper complex sits on a crystallographic inversion center. Coordinates for the amine hydrogens, H12A and H12B, were allowed to refine. Compound **10**: Data were collected on a SMART 1000 at 100 K. The copper complex sits on a crystallographic inversion center. Both 2-fluorobenzoates existed in two nearly superimposable rotamers, differing in the relative placement of the fluorine substituent. The two amine hydrogens, H22A and H22B, were placed in idealized positions and were allowed to ride. Compound **11**: Data were collected on a SMART APEX at 100 K. The copper complex sits on a crystallographic inversion center. The asymmetric unit contains a nearly superimposed disordered solvent pair of ethanol and acetonitrile. Occupancies for these two species were allowed to refine during initial model refinement and were fixed at 0.3 and 0.4 for final cycles. Coordinates for the amine hydrogens, H12A and H12B, were allowed to refine. Compound **12**: Data were collected on a SMART 1000 at 100 K. The copper complex sits on a crystallographic inversion center. Both 2-fluorobenzoates existed in two nearly superimposable rotamers, differing in the relative placement of the fluorine substituent. The (nonsymmetric) acetylene molecule sits on a crystallographic inversion center, with the 2-amino substituent having 50% site occupancy. The amino hydrogens were located in calculated positions and were allowed to ride. Compound **13**: Data were collected on a SMART APEX at 100 K. The copper complex sits on a crystallographic inversion center. The (nonsymmetric) acetylene molecule sits on a crystallographic inversion center, with the 2-amino substituent having 50% site occupancy. The amino hydrogens were located in calculated positions and were allowed to ride.
- SMART v5.060, Bruker Analytical X-ray Systems, Madison, WI, 1997–1999.
- SAINT v6.02, Bruker Analytical X-ray Systems, Madison, WI, 1997–1999.
- SHELXTL v5.10, Bruker Analytical X-ray Systems, Madison, WI, 1997.
- K. Sonogashira, Y. Tohda and N. Hagihara, *Tetrahedron Lett.*, 1975, **16**, 4467.